Annual Journal of Hydraulic Engineering, JSCE, Vol.53, 2009, February

NUMERICAL SIMULATION OF SLOSHING IN TWO DIMENSIONAL RECTANGULAR TANKS WITH SPH

Yan CUI [1], Hua LIU [2]

[1] Member of JSCE, Ph.D student, Dept. of Civil Engineering, Ritsumeikan University.(Noji Higashi 1-1-1, Kusatsu, Shiga 525-8577, Japan)

[2]Dr. of Eng., Professor, School of Naval Architecture Ocean and Civil Engineering, Shanghai Jiao Tong University(Dongchuan Road 800, Shanghai, 200240, China)

Sloshing in liquid natural gas (LNG) tankers includes extremely large deformations of the free surface. To better understand such deformations, we simulated the surge and pitch phenomenon in a two-dimensional tank using smoothed particle hydrodynamics (SPH) method. The resulting free surface elevation at tank boundary agreed closely with literature data when the tank had surge excitation. When the excitation frequency approached the highest natural frequency, impulsive pressure on the top of the tank and wave breaking appears. When the surge-pitch motions were coupled and had zero phase difference, the wave elevations were smallest. Conversely, when the coupled motions had 180degrees phase difference, the wave elevations were highest. The SPH method appears useful for understanding sloshing.

Key Words **:** *SPH method, two dimensional rectangular tank, surge, pitch, coupled effects*

1. INTRODUCTION

Sloshing induced by the motion of tanks involves extremely complete nonlinear water motions such as waves breaking, waves overturning, hydraulic jumps and so on. SPH method is a meshfree, Lagrangian, particle method that can naturally handle problems with large deformation and free surface[1)]. Thus, SPH method have been applied widely in fluid mechanics: Monaghan et at showed the applicability of SPH when applied to different free surface flow problems with waves breaking, such as breaking dams[2)], solitary waves traveling onto a beach[3)], weighted box sinking rapidly into a wave tank[4)] and so on. Oger et al[5)] presented the test cases of wedge water entries aiming at an accurate numerical simulation of solid-fluid coupling in a free surface flow. Tulin and Landrini[6)] focused on the ship-generated waves and showed the SPH's advantage of high resolution, and sufficient to capture breaking.

Many papers have reported on the sloshing phenomenon in a two-dimensional rigid rectangular tank undergoing periodic horizontal, vertical, and roll excitations. Frandsen[7)] introduced a fully non-linear finite difference model to analyze the sloshing wave motion in a 2-D tank which is moved both horizontally and vertically. Faltinsen et al[8)] used a discrete infinite-dimensional modal system in which the free surface motion and velocity potential are expanded in generalized Fourier series. This general multidimensional structure of the equations is approximated to analyze sloshing in a rectangular tank with finite water depth. Guillot[9)] applied a Runge-Kutta discontinuous Galerkin (RKDG) finite element method to the liquid sloshing problems restricted to shallow water. Chen[10)] used a time-independent finite-difference method to intensively study the combined effects of surge, heave, and pitch motions on sloshing viscous fluid. All these models are successful to simulate sloshing problems but they are invalid when either overturning waves or wave breaking appear.

In this paper SPH models for the study of nonlinear sloshing in a two-dimensional rectangular tank are presented. This model shows its applicability in simulating the phenomenon of the impacts on ceils of the tanks and wave breaks. The effects of phase differences between pitch and surge excitations are discussed.

2. SPH MODEL

(1) Governing equations

The governing equations for inviscid fluid dynamics are the Euler equations. If the Greek superscripts α and β are used to denote the coordinate directions, the Euler equations for a parcel of fluid are:

$$\frac{d\rho}{dt} = -\rho \frac{\partial \mathbf{v}^{\beta}}{\partial \mathbf{x}^{\beta}}, \tag{1}$$

$$\frac{d\mathbf{v}^{\alpha}}{dt} = \mathbf{F}^{\alpha} - \frac{1}{\rho}\frac{\partial p^{\alpha\beta}}{\partial \mathbf{x}^{\beta}}, \tag{2}$$

where d/dt indicates the Lagrangian derivative, ρ is the fluid particle density, t is time, $\mathbf{v}$ is the particle velocity, p is the fluid pressure, and $\mathbf{F}^{\alpha}$ is the body force.

To transform the above continuous fluid parameters to discrete values, by the smoothing kernel function $W(\mathbf{r} - \mathbf{r}', h)$, the integral interpolation of any function $A(\mathbf{r})$ is defined approximately by[11]

$$A(\mathbf{r}) = \int_{\Omega} A(\mathbf{r}') W(\mathbf{r} - \mathbf{r}')\, d\mathbf{r}', \tag{3}$$

where A is supposed to be smoothed in the area Ω, h is the smoothing length defining the influence area of W. Because of the compact support of W, the spatial derivative of A can be approximately converted to the derivative of the kernel function:

$$\nabla A(\mathbf{r}) = \int_{\Omega} A(\mathbf{r}') \nabla W(\mathbf{r} - \mathbf{r}', h)\, d\mathbf{r}'. \tag{4}$$

Using the above concepts, any quantity $A(\mathbf{r})$ of particle i, whether scalar or vector, can be approximated by the direct summation of the relevant quantities over its neighboring particles, denoted by j

$$A(\mathbf{r}_i) = \sum_{j=1}^{N} m_j \frac{A_j}{\rho_j} W(|\mathbf{r}_i - \mathbf{r}_j|, h). \tag{5}$$

Similar the derivative of $A(\mathbf{r})$ can be expressed as

$$\nabla A(\mathbf{r}_i) = \sum_{j=1}^{N} m_j \frac{A_j}{\rho_j} \nabla W(|\mathbf{r}_i - \mathbf{r}_j|, h). \tag{6}$$

Then the SPH formulation of governing equations (1) and (2) can be written

$$\frac{d\rho_i}{dt} = \sum_{j=1}^{N} m_i v_{ij}^{\beta} \frac{\partial W_{ij}}{\partial x_i^{\beta}}, \tag{7}$$

$$\frac{dv_i^{\alpha}}{dt} = F_i^{\alpha} - \sum_{j=1}^{N} m_i \left(\frac{p_i}{\rho_i^2} + \frac{p_j}{\rho_j^2} + \Pi_{ij} \right) \cdot \frac{\partial W_{ij}}{\partial x_i^{\beta}}, \tag{8}$$

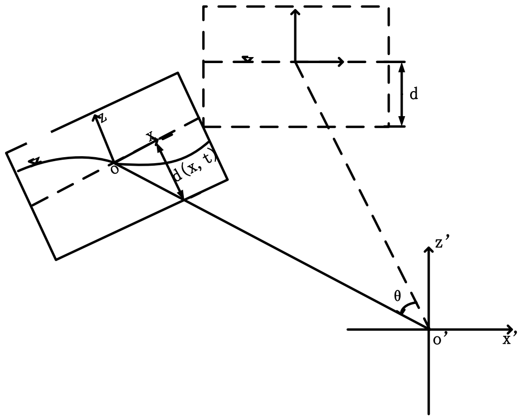

Fig. 1 Definition sketch of coordinate system

where $v_{ij}^{\beta} = v_i^{\beta} - v_j^{\beta}$, and Π_{ij} is an artificial viscosity term that stabilize the numerical algorithm[12]:

$$\Pi_{ij} = \begin{cases} \dfrac{-\alpha_{\Pi} c_{ij} \Phi_{ij} + -\beta_{\Pi} \Phi_{ij}^2}{\rho_{ij}} & \mathbf{v}_{ij} \cdot \mathbf{r}_{ij} \geq 0 \\ 0 & \mathbf{v}_{ij} \cdot \mathbf{r}_{ij} < 0 \end{cases}, \tag{9}$$

where

$$\Phi_{ij} = \frac{k_1 + k_2}{2} \frac{h_{ij} \mathbf{v}_{ij} \cdot \mathbf{r}_{ij}}{|\mathbf{r}_{ij}|^2 + \phi_{ij}^2}, k_i = \frac{|\mathrm{div}\,\mathbf{v}_i|}{|\mathrm{div}\,\mathbf{v}_i|^2 + |\mathrm{curl}\,\mathbf{v}_i| + 10^{-4} \dfrac{c_i}{h}},$$

$$c_{ij} = \frac{1}{2}(c_i + c_j), \quad \rho_{ij} = \frac{1}{2}(\rho_i + \rho_j),$$

$$h_{ij} = \frac{1}{2}(h_i + h_j), \quad \mathbf{v}_{ij} = \mathbf{v}_i - \mathbf{v}_j, \qquad \mathbf{r}_{ij} = \mathbf{r}_i - \mathbf{r}_j,$$

$$\alpha_{\Pi} = 0.01, \quad \beta_{\Pi} = 0.$$

The use of different kernels in SPH is the analogue of using different difference schemes in finite difference methods. Colagrossi et al[12] introduced a new highly stable kernel that is computationally efficient:

$$W(|\mathbf{r}|, h, \delta) = \frac{e^{-\left(\frac{|\mathbf{r}|}{h}\right)^2} - e^{-\left(\frac{\delta}{h}\right)^2}}{2\pi \int_0^{\delta} |\mathbf{r}| \left(e^{-\left(\frac{|\mathbf{r}|}{h}\right)^2} - e^{-\left(\frac{\delta}{h}\right)^2} \right) d|\mathbf{r}|}, \tag{10}$$

where $|\mathbf{r}|$ is the distance between two particles, $\delta = 3h$.

Let o'x'z' be an absolute coordinate system and oxz is a coordinate system that moves with the tank (Fig. 1). If the length of the tank is l, height of the tank is *H*, unperturbed depth of the water is *d*,, according to the linear theory[13], the *n*th natural frequency of fluid oscillations in the tank is

$$\omega_n = \sqrt{g \frac{n\pi}{l} \tanh\left(\frac{n\pi}{l} d \right)}, \tag{11}$$

where n=1, 2, 3$\cdots$.

We specify a forcing of surge and pitch according to ：

$$x_s(t) = A_s \sin(\omega_s t + \varepsilon_s), \quad (12)$$

$$\theta_p(t) = \theta_0 \sin(\omega_p t + \varepsilon_p), \quad (13)$$

where x_s is the displacement of the surge excitations, A_s and θ_0 are the amplitudes of surge and pitch,, respectively, ω_s and ω_p are the surge and pitch frequencies, ε_s and ε_p are the initial phases of surge and pitch, θ_p is the angular displacement of pitch.

In coordinates that are fixed relative to the moving tank, the body forces can be written as

$$F_i^1 = -g\sin\theta_p + z_i\ddot{\theta}_p + x_i\dot{\theta}_p^2 + 2\dot{\theta}_p w_i - \ddot{x}_s, \quad (14)$$

$$F_i^2 = -g\cos\theta_p - x_i\ddot{\theta}_p + z_i\dot{\theta}_p^2 + 2\dot{\theta}_p u_i, \quad (15)$$

Where F_i^1 and F_i^2 are the components of body force on particle i in the x-direction and z-direction, g is the acceleration of gravity,, x_i and u_i are the displacement and velocity at particle i in the x-direction, whereas z_i and w_i are the corresponding displacement and velocity at particle i in the z-direction. Guillot[9], Chen[10], Huang[14] and Celebi and Akyildiz[15] adopted similar expressions.

(2) Equation of State

Here we consider the fluid flow as compressible and use the equation of state proposed by Monaghan[2]:

$$p = B\left[\left(\frac{\rho}{\rho_0}\right)^{\gamma} - 1\right], \quad (16)$$

where $\gamma = 7$ and $\rho_0 = 1000$ for water. The parameter B is chosen to keep the amplitude of density oscillations around the reference density ρ_0 less than 1 %.

(3) Boundary Conditions

We adopted the treatment approach proposed by Gong[16] to determine pressure at a solid boundary (Fig. 2). The boundary is built with three layers of fixed particles: a layer of boundary particles on the solid wall and two layers of virtual particles outside the solid wall. The pressure of the boundary particles is used to solve the momentum equations at the fluid particles near the boundary. Pressures of the boundary particles are obtained through the following approach. For a given boundary particle B, its pressure is obtained by interpolation using the pressure of fluid particles in the near-boundary area around B that can be imagined as a pressure "sensor" during an experiment. Only the fluid particles that lie within a distance d (set proportional to the smoothing length) from the boundary and within the projected cylinder of the "sensor" S_{Sensor} are used to estimate the pressure of point B. First, we project the fluid particles to S_{Sensor}. The pressure of the projected point P_{j1}' is obtained from the fluid particle P_{j1} considering the hydrostatic pressure due to the vertical distance Δd between the particle and its projection, i.e. $P_{j1}' = P_{j1} + \rho g \Delta d$. Secondly, S_{Sensor} is divided into N parts whose characteristic length is proportional to smoothing length. Assuming the area of the i th part is dS_i, the pressure P_i at i th part is the average of the pressure P_{j1}' of all the projected points in part dS_i. Then the pressure P_B at particle B is taken as

$$p_B = \frac{\sum_i p_i dS_i}{\sum_i dS}. \quad (17)$$

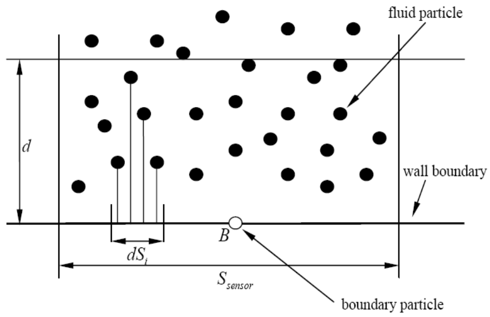

Fig. 2 Boundary treatment

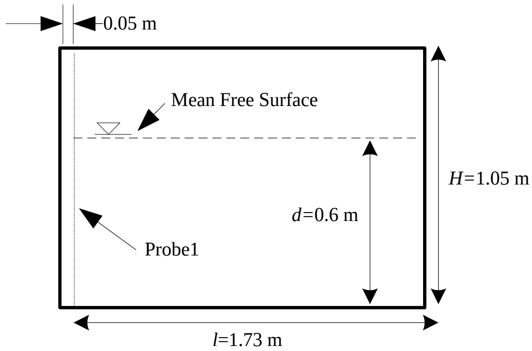

Fig. 3 Tank dimensions and wave probe positions

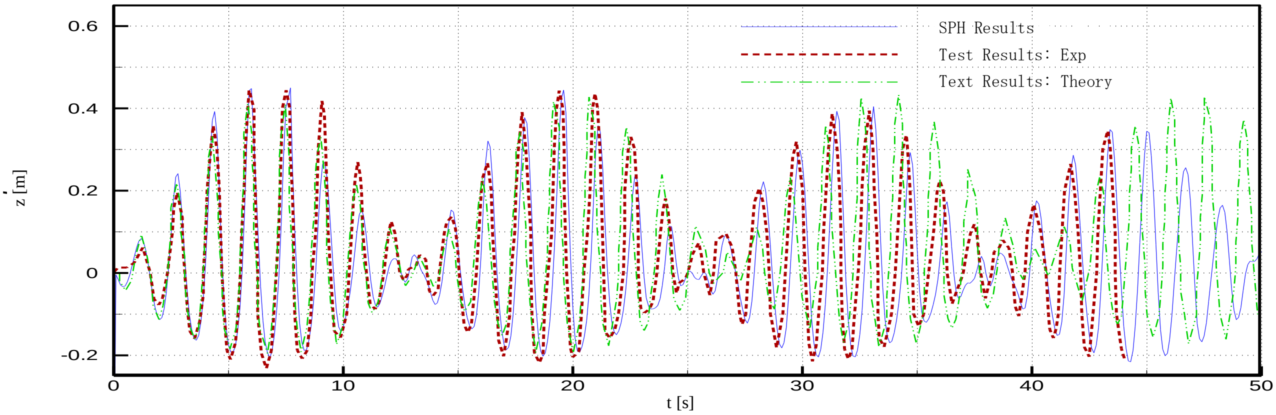

Fig. 4 Free surface elevation at wave probe at Probe1 when A_s =0.032 m, $w_s = 0.9\ w_1$ (Compared with Faltinsen et al's results[8])

(4)Time Integration

The discrete SPH equations above are integrated in time by the Leap-Frog (LF) method. The advantage of the LF algorithm is its low memory storage requirement in the computation and the efficiency for one force evaluation per step:

$$\mathbf{v}^{t+\frac{1}{2}\Delta t} = \mathbf{v}^{t} + \frac{1}{2}\Delta t\left(\frac{\mathbf{v}^{t-\frac{1}{2}\Delta t}}{dt}\right), \tag{18}$$

$$\mathbf{v}^{t+\Delta t} = \mathbf{v}^{t} + \Delta t\left(\frac{\mathbf{v}^{t+\frac{1}{2}\Delta t}}{dt}\right). \tag{19}$$

3. NUMERICAL SIMULATION OF SURGE

In this section, simulation results for nonlinear sloshing in a smooth rectangular tank due to horizontal excitation are compared with the experimental and theoretical results given by Faltinsen et al[8) .

(1)Parameters and Particles Distribution

As shown in Fig. 3, l is 1.73 m, H is 1.05 m and d is 0.6 m. According to equation (11) the highest natural frequency is ω_1 = 3.76 Hz. A wave probe was placed 0.05 m from the left wall. The origin of the coordinate system was at the lower left corner. The computational domain was 0 $\le x \le$ 1.73 m, 0 $\le z \le$ 1.05 m. The initial separation between the fluid particles in the x and z directions were both 0.01 m, and 10380 fluid particles and 1702 boundary particles were used in the simulations. A constant time step of 5×10^{-5} s was used; for a 50-s-long series of 1×10^{6} time steps, it took about 120 hours using an AMD Athlon64x2 4000+ CPU.

(2)Numerical Test

We set A_s = 0.032 m and $\omega_s = 0.9\omega_1$ to match the conditions of Faltinsen et al[8)]'s experimental results. According to Fig. 4, the free surface elevation at Probe1 is in good agreement with their experimental results. Comparison with inviscid theoretical results suggests however that dissipation reduces the amplitude in the third and fourth "wave packet". Accordingly, it is likely that the good agreement with experiment depends on a

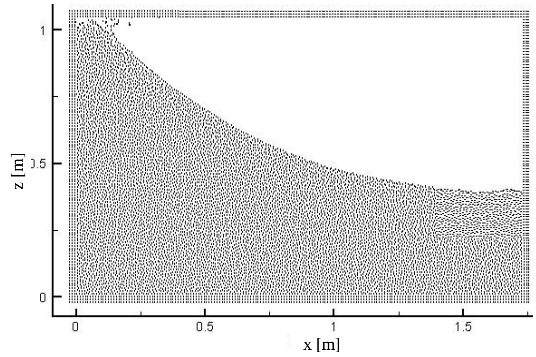

Fig. 5 Water impact on top ceiling

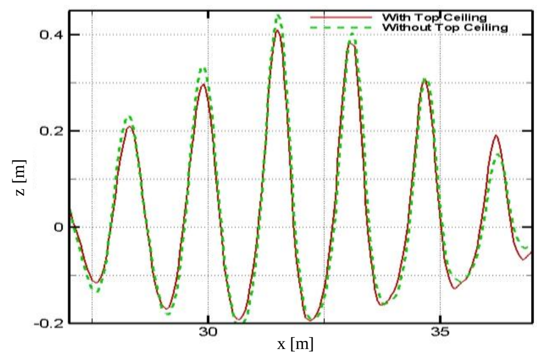

Fig. 6 Free surface elevations in tanks with and without top ceiling

fortuitous choice of the parameters in the artificial viscosity term in our SPH simulation. Also during the third and fourth "wave packet", phase shifts between our results and experimental data can be observed. This kind of shifts always happens when the wave amplitudes are small. We can also see the phase difference between Faltinsen et al[8]'s and theoretical results, and it is visible that our SPH results have less shifts from the experiment comparing to Faltinsen et al[8]'s theoretical results. As shown in Fig. 5, when water impacts on the ceiling, the free surface overturns and some water particles splash down. Fig. 6 compares the surface elevation between tanks with and without a top ceiling during one "wave packet". It is evident that they do not agree near the peaks of the "packets" (nearly 5% difference), where the water impacts on the ceiling (as shown in Fig. 5) happened. All these figures show that when a forceful impact occurs, the numerical dissipation of the SPH method becomes significant.

4.COUPLED SURGE AND PITCH MOTION

(1) Parameters and Particles Disposition

We adopted the same tank that was used to simulate the surge motions (Fig. 3). A_s = 0.005 m, $\omega_s = 0.95\omega_1$, $\theta_0 = 1^\circ$, $\omega_p = 0.9\omega_1$. 5 cases are considered: pure surge excitation, pure pitch excitation, coupled excitations when phase difference is 0°,、coupled excitations when phase difference is 90° and coupled excitations when phase difference is 180°.

(2) Analyses of the results

Fig. 7 demonstrates the free surface elevation at the probe under different excitations, peaks of the envelope appear near t=16 s. While considering the coupled excitations of surge and pitch (Fig. 7 (c)(d)(e)), the results are different from the linear superposition of pure surge and pure pitch, which indicates the nonlinearity of sloshing. When the phase difference is 0°, the amplitude is smallest, and smaller than the superposition of the two single excitation cases, meaning that the couple effect is negative. By contrast, when the phase difference is 90 degrees, the elevation is almost the same as the two single excitation cases, which means the coupling effect is week. Finally when the phase difference is 180 degrees, the elevation reaches up to 0.2 m, the couple effective is positive. (The difference between the (d) and (e) in Fig. 7 is not very obvious because of the different vertical

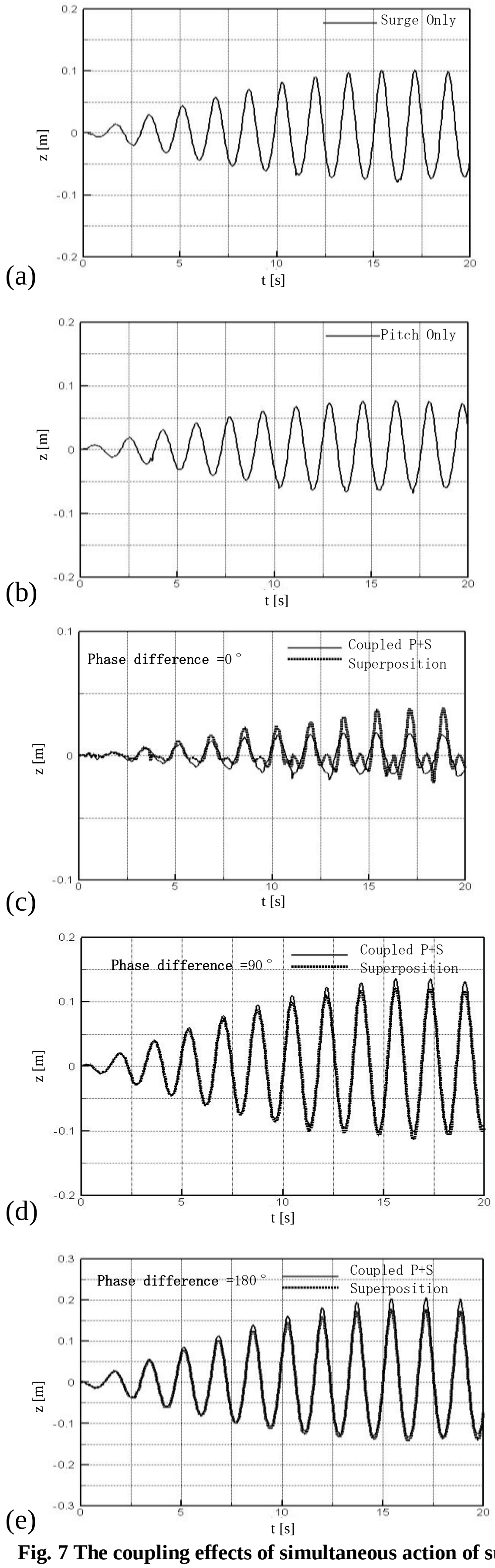

Fig. 7 The coupling effects of simultaneous action of surge and pitch motions (With different vertical scales)

scales.) So for a tank under surge excitation, if we can supply an artificial pitch excitation with a proper phase difference, the motions of the liquid in the tank can be significantly promoted or suppressed. It is supposed to be more efficient than supplying an artificial surge exciting because of the nonlinearity.

5. CONCLUSION

Simulation of SPH to the surge and pitch motions in a two dimensional rectangular tank is presented in this paper. The case of surge shows a good agreement with literature results[8)]. When the exciting frequency is near the highest natural frequency, the simulation demonstrates the phenomenon of wave breaking and water particles splash , which is caused by the wave impacts on the ceiling, and the effect of the impacts to the numerical results is discussed. The simulation of coupled surge-pitch exciting illustrates the effects of the phase differences. The elevation is smallest when phase difference is 0° and largest when phase difference is 180°. The effect of the coupling is nonlinear. When phase difference is 90°, the coupling effect is not obvious.

The SPH method has shown its advantage when applied to sloshing problems with large deformation of free surface. But further work is still needed to decrease the numerical dissipation and to improve the computational efficiency during long computational periods._In the future SPH method should be easily applied to many other sloshing problems such as sloshing in 3-D and complex geometries tanks, sloshing in elastic tanks and so on.

REFERENCES

1) Du, X. T., Wu, W., Gong, K. and Liu, H.: Two-dimensional SPH simulation of water waves generated by underwater landslide, *Journal of Hydrodynamics (Ser .A)*, 21(5): 579-586, 2005.
2) Monaghan, J. J.: Simulating free surface flow with SPH, *Journal of Computational Physics*, 110: 399-406, 1994.
3) Monaghan, J. J. and Kos, A.: Solitary waves on a Cretan beach, *Journal of Waterway, Port, Coastal and Ocean Engineering, ASCE*, 125(3): 145-154, 1999.
4) Monaghan, J. J.: SPH without a tensile instability, *Journal of Computational Physics*, 159: 290-311, 2000.
5) Oger, G., Doring, M., Alessandrini, B. and Ferrant P.: Two-dimensional SPH simulations of wedge water entries, *Journal of Computational Physics*, 213: 803-822, 2006.
6) Tulin, M. P. and Landrini, M.: Breaking waves in the ocean and around Ships, *Proceedings of 23rd ONR Symposium on Naval Hydrodynamics*, 713-745, Val de Reuil, France, 2000.
7) Frandsen J. B.: Sloshing motions in excited tanks, *Journal of Computational Physics*, 196: 53-87, 2004.
8) Faltinsen, O. M., Rognebakke, O. F., Lukovsky, I. A. and Timokha, A. N.: Multidimensional modal analysis of nonlinear sloshing in a rectangular tank with finite water depth, *Journal of Fluid Mechanics*, 407: 201-234, 2000.
9) Guillot, M. J.: Application of a Discontinuous Galerkin Finite Element Method to Liquid Sloshing, *Journal of Offshore Mechanics and Arctic Engineering*, 128(1): 1-10, 2006.
10) Chen, B. F.: Viscous fluid in tank under coupled surge, heave, and pitch motions, *Journal of Waterway, Port, Coastal, and Ocean Engineering*, 131(5): 239-256, 2005.
11) Liu, G. R. and Liu, M. B.: *Smoothed Particle Hydrodynamics: a Meshfree Particle Method*, World Scientific, 2003.
12) Colagrossi, A. and Landrini, M.: Numerical simulation of interfacial flows by smoothed particle hydrodynamics, *Journal of Computational Physics*, 191: 448-475, 2003.
13) Zhu, R. Q.: Time domain simulation of liquid sloshing and its interaction with flexible structure, Wuxi, Jiangsu, China Ship Scientific Research Center , 2002.
14) Huang, T. C.: *Engineering Mechanics, vol. II, Dynamics,* Addison-Wesley Publishing Company Inc., 1967.
15) Celebi, M. S. and Akyildiz, H.: Nonlinear modeling of liquid sloshing in a moving rectangular tank, *Ocean Engineering*, 29 (12): 1527–1553, 2002.
16) Gong, K. and Liu, H.: A new boundary treatment for smoothed particle hydrodynamics, *Asian and Pacific Coast,* Nanjing, China,2007

(Received September 30, 2008)